Optics and Lasers in Engineering 47 (2009) 484–487

Contents lists available at ScienceDirect

Optics and Lasers in Engineering

journal homepage: www.elsevier.com/locate/optlaseng

Full-field measurement of the phase retardation for birefringent elements by using common path heterodyne interferometry

Yen-Liang Chen, Der-Chin Su *

Department of Photonics, Institute of Electro-Optical Engineering, National Chiao-Tung University, 1001 Ta-Hsueh Road, Hsinchu 300, Taiwan

ARTICLE INFO

Available online 27 June 2008

Keywords:
Electro-optic modulation
Phase retardation
Heterodyne interferometry
Common-path interferometry

ABSTRACT

A collimated heterodyne light passes through the tested material and an analyzer, full-field interference signals are taken by a fast CMOS camera. The series of interference intensities recorded at any pixel are the sampling points of a sinusoidal signal. From those points, the associated argument of that pixel can be derived by a least-square sine fitting algorithm on IEEE 1241 Standards. Subtracting the average argument of the reference signal, the phase retardation of that pixel can be obtained. The phase retardations of other pixels can be obtained similarly. Its validity is demonstrated.

1. Introduction

The birefringent material is often used in optical systems. Its phase retardation strongly affects their functions. So it is necessary to measure its phase retardation accurately. Several methods were proposed to measure the phase retardation [1–11], and they have good measured results. Except Lo's method [11], they are valid only for one point measurement. Although Lo's method is suitable for measuring the full-field phase retardation of the birefringent material, it uses the integrating-bucket method which is similar to the phase-shifting technique [12]. To improve the measurement accuracy, an alternative method for measuring full-field phase retardation is proposed in this paper. A collimated heterodyne light passes through the tested material and an analyzer, full-field interference signals are taken by a fast CMOS camera. The series of interference intensities recorded in any pixel are the sampling points of a sinusoidal signal. From those points, the associated argument of the pixel can be derived by a least-square sine fitting algorithm on IEEE 1241 Standards [13]. Subtracting the average argument of the reference signal, the phase retardation of the pixel can be obtained. The phase retardations of other pixels can be calculated similarly. To show the validity of this method, a quarter wave-plate is tested. This method has both merits of the common-path interferometry and the heterodyne interferometry.

2. Principle

2.1. The intensities of the reference signal and the test signal

The schematic diagram of this method is shown in Fig. 1. A linearly polarized light passes through an electro-optic (EO) modulator driven by a function generator (FG). A saw-tooth signal with frequency f and half-voltage amplitude $V_{\lambda/2}$ is applied to the EO modulator. The light beam is collimated by an optical module that consists of a microscopic objective (MO), a pinhole (PH) and a collimating lens (CL). Next, the collimated light passes through a polarizer (P), a test sample (S), an analyzer (AN), and an imaging lens (IL), and finally enters a CMOS camera (C). The S is a common used circular wave-plate, and it is imaged by the IL. The image of the S is located on the plane of the CMOS camera, which is represented as Region I. The other area on the plane of the CMOS camera is represented as Region II, as shown in Fig. 2. If the light amplitudes of the pixels in the Region I and the Region II are E_t and E_r, then their intensities are $I_t = |E_t|^2$ and $I_r = |E_r|^2$. Here I_t and I_r act as a test signal and a reference signal, respectively.

For convenience, the $+z$-axis is chosen along the light propagation and the y-axis is along the vertical direction. Let the laser light be linearly polarized at 45° with respect to the x-axis and both the fast axes of the EO modulator and the S be along the x-axis. If the transmission axes of the P and the AN are located at 45° with respect to x-axis, then the Jones vectors of E_t and E_r can be derived and written as [14]

$$\begin{aligned} E_t &= \mathrm{AN}\times \mathrm{S}\times \mathrm{EO}\times E_o \\ &= \frac{1}{2}\begin{pmatrix}1 & 1\\ 1 & 1\end{pmatrix}\begin{pmatrix}e^{i(\psi/2)} & 0\\ 0 & e^{-i(\psi/2)}\end{pmatrix}\begin{pmatrix}e^{i\pi ft} & 0\\ 0 & e^{-i\pi ft}\end{pmatrix}\frac{1}{\sqrt{2}}\begin{pmatrix}1\\ 1\end{pmatrix}e^{i2\pi f_0 t} \\ &= \frac{1}{2\sqrt{2}}\begin{pmatrix}e^{i(2\pi ft+\psi/2)}+e^{-i(2\pi ft+\psi/2)}\\ e^{i(2\pi ft+\psi/2)}+e^{-i(2\pi ft+\psi/2)}\end{pmatrix}e^{i2\pi f_0 t} \end{aligned} \quad (1)$$

and

$$\begin{aligned} E_r &= \mathrm{AN}\times \mathrm{EO}\times E_o \\ &= \frac{1}{2}\begin{pmatrix}1 & 1\\ 1 & 1\end{pmatrix}\begin{pmatrix}e^{i\pi ft} & 0\\ 0 & e^{-i\pi ft}\end{pmatrix}\frac{1}{\sqrt{2}}\begin{pmatrix}1\\ 1\end{pmatrix}e^{i2\pi f_0 t} \end{aligned}$$

* Corresponding author. Tel.: +886 3 5731951; fax: +886 3 5716631.
E-mail address: t7503@faculty.nctu.edu.tw (D.-C. Su).

0143-8166/$ - see front matter © 2008 Elsevier Ltd. All rights reserved.
doi:10.1016/j.optlaseng.2008.05.012

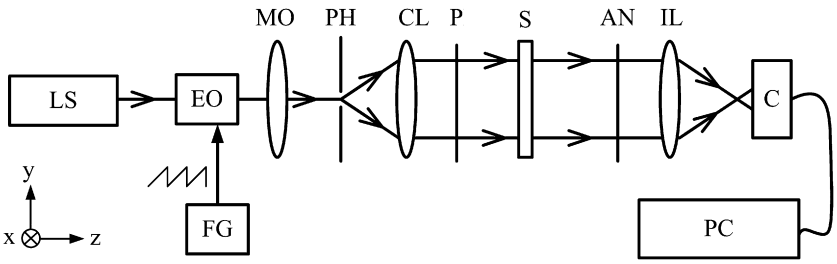

Fig. 1. Schematic diagram for measuring the full-field phase retardation of a wave-plate. LS: laser light source; EO: electro-optic modulator; FG: function generator; MO: microscopic objective; PH: pinhole; CL: collimated lens; P: polarizer; S: sample; AN: analyzer; IL: imaging lens; C: CMOS camera; PC: personal computer.

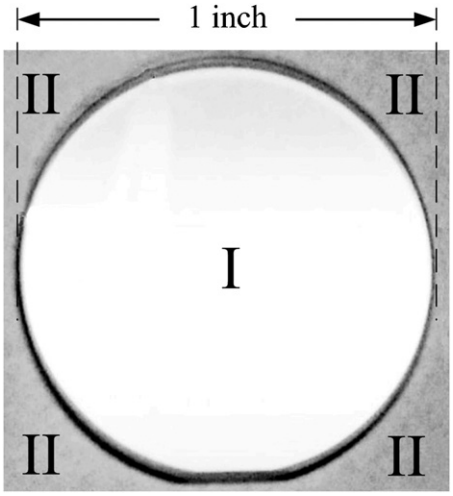

Fig. 2. The image (Region I) of a circular wave plate in the square image plane of the camera.

$$= \frac{1}{2\sqrt{2}} \begin{pmatrix} e^{i(2\pi ft/2)} + e^{-i(2\pi ft/2)} \\ e^{i(2\pi ft/2)} + e^{-i(2\pi ft/2)} \end{pmatrix} e^{i2\pi f_0 t}, \tag{2}$$

where f_0 means the light frequency and ψ is the phase retardation caused by the S. The associated intensities can be expressed as

$$I_t = \tfrac{1}{2}[1 + \cos(2\pi ft + \psi + \phi_r)] \tag{3}$$

and

$$I_r = \tfrac{1}{2}[1 + \cos(2\pi ft + \phi_r)], \tag{4}$$

where ϕ_r is the initial phase. Since both of them are sinusoidal signals, they can be rewritten in the form as

$$I_t = A_t \cos(2\pi ft) + B_t \sin(2\pi ft) + C_t \tag{5}$$

and

$$I_r = A_r \cos(2\pi ft) + B_r \sin(2\pi ft) + C_r, \tag{6}$$

where A_t, B_t, C_t, A_r, B_r and C_r are real numbers. Their phase difference ψ can be derived and written as

$$\psi = \psi_t - \psi_r = (\psi + \phi_r) - \phi_r = \tan^{-1}\left(\frac{-B_t}{A_t}\right) - \tan^{-1}\left(\frac{-B_r}{A_r}\right), \tag{7}$$

where ψ_t and ψ_r are the measured phases in the Regions I and II, respectively. From Eq. (7), it is obvious that ψ can be estimated under the conditions when A_t, B_t, A_r and B_r are specified. In order to enhance measurement accuracy in our research, ψ_r is the average value of the phase for all the pixels in the Regions II.

2.2. Phase estimation

A CMOS camera with frame frequency f_c is used to take n frames in a recording time, so every pixel records a series of n interference intensities, which are the sampled points of a sinusoidal signal, as shown in Fig. 3. According to Nyquist sampling theorem [15], the condition $f_c \geqslant 2f$ should be valid to avoid aliasing. If n interference intensities recorded by any pixel at time $t_1, t_2, \ldots, t_n$ are $I_1, I_2, \ldots, I_n$, then we have

$$\begin{pmatrix} I_1 \\ I_2 \\ \vdots \\ I_n \end{pmatrix} = M \times \begin{pmatrix} A \\ B \\ C \end{pmatrix},$$

where

$$M = \begin{pmatrix} \cos\omega t_1 & \sin\omega t_1 & 1 \\ \cos\omega t_2 & \sin\omega t_2 & 1 \\ \vdots & \vdots & \vdots \\ \vdots & \vdots & \vdots \\ \cos\omega t_n & \sin\omega t_n & 1 \end{pmatrix}. \tag{8}$$

A, B and C can be derived by using a least-square fitting algorithm on IEEE Standards [13] and they can be expressed as

$$\begin{pmatrix} A \\ B \\ C \end{pmatrix} = (M^t M)^{-1} M^t \begin{pmatrix} I_1 \\ I_2 \\ \vdots \\ I_n \end{pmatrix}, \tag{9}$$

where M^t means the transpose matrix of M. Next substituting the estimated data of A and B into Eq. (7), the phase retardation of that pixel can be calculated. If these processes are applied to other pixels, then their phase retardations can be obtained similarly.

3. Experiment and result

To demonstrate the validity of this method, an He–Ne laser with 632.8 nm wavelength, an EO modulator (New Focus/Model 4002), and a CMOS camera (Basler/A504 K) with 8-bit gray level and 320×256 pixel image resolution are used to test a commercial zero-order quartz quarter-wave plate (Union Optic/WPF4125) [16] with $(n_e, n_o) = (1.553, 1.544)$, $d = 17.58\,\mu m$ effective thickness (only the thickness of the quartz crystal, not including the thickness of the substrate glass) and 1 in. diameter is tested. Here n_e and n_o are the extraordinary and ordinary refractive indices, respectively. Under the conditions $f = 100$ Hz, $V_{\lambda/2} = 144$ V, $f_c = 1499.3$ frames/s, $n = 300$ frames are taken in 0.2 s. The

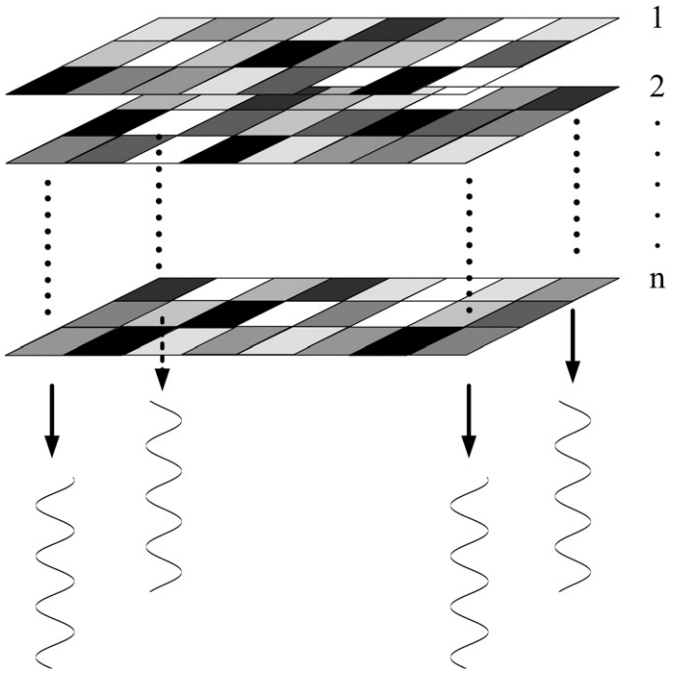

Fig. 3. A series of n interference intensities recorded by every pixel.

condition $f_c = 1499.3$ frames/s is chosen based on the optimal condition proposed by Jian et al. [17] to decrease the measurement error. Next, a least-square sine fitting algorithm on IEEE 1241 Standards in a MATLAB program is utilized to estimate the data of ψ of every pixel. The measured full-field phase retardation is shown in gray scale in Fig. 4. The average phase retardation is 1.573 rad, and one-dimensional phase retardation distribution along the dotted line in Fig. 4 is shown in Fig. 5. From Fig. 5, it can be seen that the measured results near the periphery are strongly influenced by the edge diffraction. In addition, the deviation (i.e., the difference between the measured result and the average value 1.573 rad) distribution corresponding to the square part labeled in the dotted line in Fig. 4 is calculated and depicted in Fig. 6. The associated standard deviation is 0.030 rad.

4. Discussion

From Eq. (7), it is obvious that both ψ_t and ψ_r should be within the range $(-\pi/2, \pi/2)$. If the polarities (positive or negative) of A_t, B_t, A_r and B_r are considered to determine the associated quadrants, then the range of ψ_t and ψ_r can be expanded as $(-\pi, \pi)$. Consequently, ψ may be within the range $(-2\pi, 2\pi)$ according to Eq. (7). If ψ is not within the range $(-\pi, \pi)$, it should be modified by using the similar operation in the phase unwrapping process [18]. That is, -2π and 2π are added to ψ, respectively; only one result is within the range $(-\pi, \pi)$. The modified result is the phase retardation to be measured.

The errors in the phase difference measurement in this technique may be influenced by the following factors:

(1) *Collimating error*
It depends on the collimation quality of the light beam. The central part of the light beam is incident on the test waveplate normally, and the peripheral part is incident with the incident angle $\Delta\theta$. Chang's technique [19] is introduced to improve the collimation quality of the light beam, and the

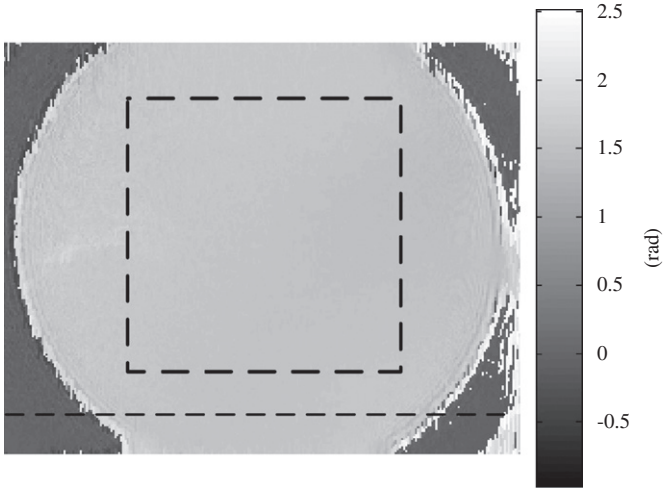

Fig. 4. The measured full-field phase retardation distribution in gray level.

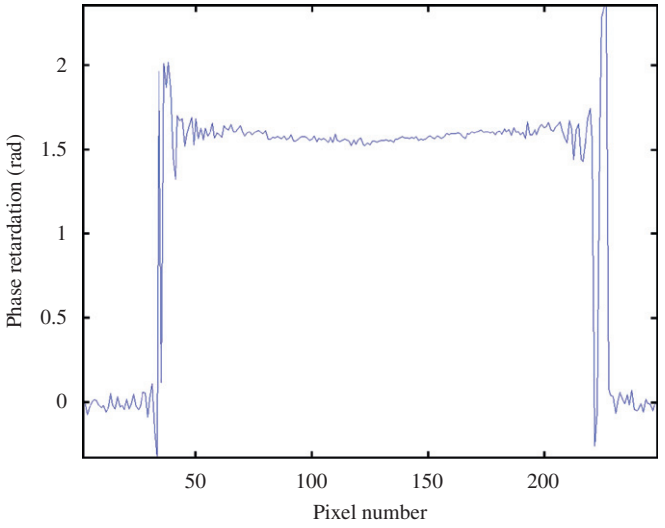

Fig. 5. One-dimensional phase retardation distribution along the dotted line in Fig. 4.

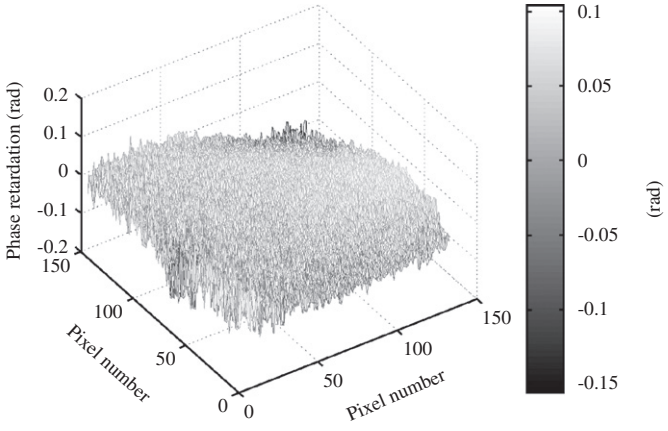

Fig. 6. The measured deviation from the average value for a square part in Fig. 4.

condition $\Delta\theta = 0.02^\circ$ can be achieved. If the angle between the propagation direction and the optical axis of the birefringent element is θ, then the effective extraordinary index $n_e(\theta)$ can

be expressed as [20]

$$\frac{1}{n_e^2(\theta)} = \frac{\cos^2\theta}{n_o^2} + \frac{\sin^2\theta}{n_e^2}. \quad (10)$$

Consequently, the associated collimating error $\Delta\phi_c$ is

$$\Delta\phi_c = \frac{[n_e(\theta) - n_o]d}{\lambda} \times 360^\circ, \quad (11)$$

where λ is the light wavelength. Substituting our experimental conditions $(n_e,\ n_o) = (1.553,\ 1.544)$, $d = 17.58\,\mu m$, $\theta = 90 \pm 0.02^\circ$ and $\lambda = 0.6328\,\mu m$ into Eqs. (10) and (11), $\Delta\phi_c \approx (1.1 \times 10^{-5})^\circ$ can be obtained. In addition, the contrast of the interference signal in Region II decreases by multiplying the factor $\cos(\Delta\theta)$. When $\Delta\theta$ is smaller than 10°, the contrast almost remains unchanged. Consequently, the measured results of the Region II are hardly influenced by the collimation quality of the light beam.

(2) *Sampling error*
It depends on the frequency of the heterodyne interference signal, the camera recording time, the frame period, the frame exposure time and the number of gray levels. The optimal condition presented by Jian et al. [17] is used in our tests, so the sampling error $\Delta\phi_s$ is about 0.036°.

(3) *Polarization-mixing error*
Owing to the extinction ratio effect of a polarizer, mixing of light polarization occurs. In our experiments, the extinction ratio of the polarizer (Japan Sigma Koki, Ltd.) is 1×10^{-5} is used. It can be estimated in advance to modify the measured results. The polarization-mixing error can be decreased to $\Delta\phi_p = 0.03^\circ$ with this modification [21].

(4) *Azimuthal angular angle*
It occurs from the misalignments between the fast axes the EO modulator and the test birefringent element. If there is an angle ε between them, then the azimuthal angular error $\Delta\phi_a$ depends on ε and ψ. It can be estimated as Chiu et al. [6] did, and we have $\Delta\phi_a \approx 0.03^\circ$ as $|\varepsilon| = 5^\circ$ at $\psi = 90^\circ$.

Consequently, the total error of this method is $\Delta\phi \approx 0.1^\circ$. In addition, this method can be applied to check the phase retardation uniformity of the sample.

5. Conclusion

In this paper, an alternative method for measuring full-field phase retardation has been proposed. A collimated heterodyne light passes through the tested material and an analyzer, full-field interference signals are taken by a fast CMOS camera. The series of interference intensities recorded at any pixel are the sampling points of a sinusoidal signal. From those points, the associated argument of that pixel can be derived. Subtracting the average argument of the reference signal, the phase retardation of that pixel can be obtained. The phase retardations of other pixels can be obtained similarly. To show the validity of this method, a quarter wave-plate has been tested. This method has both merits of the common-path interferometry and the heterodyne interferometry.

Acknowledgment

This study was supported in part by the National Science Council, Taiwan, ROC, under Contract NSC95-2221-E009-236-MY3.

References

[1] Grunstra BR, Perkins HB. A method for measurement of optical retardation angles near 90 degrees. Appl Opt 1996;5:585–7.
[2] McIntyre CM, Harris SE. Achromatic wave plates for the visible spectrum. J Opt Soc Am 1968;58:1575–80.
[3] Lin Y, Zhou Z, Wang R. Optical heterodyne measurement of the phase retardation of a quarter-wave plate. Opt Lett 1988;13:553–5.
[4] Nakadate S. High precision retardation measurement using phase detection of Young's fringes. Appl Opt 1990;29:242–6.
[5] Sypek M. A new technique for the measurement of phase retardation. Opt Laser Technol 1991;23:42–4.
[6] Chiu MH, Chen CD, Su DC. Method for determining the fast axis and phase retardation of a wave plate. J Opt Soc Am A 1996;13:1924–9.
[7] Feng CM, Huang YC, Chang JG, Chang M, Chou C. A true phase sensitive optical heterodyne polarimeter on glucose concentration measurement. Opt Commun 1997;141:314–21.
[8] Ma'rquez A, Yamauchi M, Davis JA, Franich DJ. Phase measurement of a twist nematic liquid crystal spatial light modulator with a common-path interferometer. Opt Commun 2001;190:129–33.
[9] Lo YL, Hsu PF. Birefringence measurements by an electro-optic modulator using a new heterodyne scheme. Opt Eng 2002;41:2764–7.
[10] Lo YL, Lai CH, Lin JF, Hsu PF. Simultaneous absolute measurements of principle angle and phase retardation with a new common-path heterodyne interferometer. Appl Opt 2004;43:2013–22.
[11] Lo YL, Chih HW, Yeh CY, Yu TC. Full-field heterodyne polariscope with an image signal processing method for principal axis and phase retardation measurements. Appl Opt 2006;45:8006–12.
[12] Greivenkamp JE, Bruning JH. Phase-shifting interferometers. In: Malacara D, editor. Optical shop testing. 2nd ed. New York: Wiley; 1992. p. 501–98.
[13] IEEE. Standard for terminology and test methods for analog-to-digital converters. IEEE Std 1241-2000, 2000, p. 25–9.
[14] Hecht E. Optics. 4th ed. Addison-Wesley; 2002. p. 376–9.
[15] Nyquist H. Certain topics in telegraph transmission theory. Trans AIEE 1928;47:617–44.
[16] 〈http://www.u-optic.com/wpf.htm〉.
[17] Jian ZC, Chen YL, Hsieh HC, Hsieh PJ, Su DC. Optimal condition for full-field heterodyne interferometry. Opt Eng 2007;46:115604.
[18] Osten W, Juptner W. Digital processing of fringe patterns in optical metrology. In: Rastogi PK, editor. Optical measurement techniques and applications. Norwood: Artech House Inc.; 1997. p. 72–6.
[19] Chang CW, Su DC, Chang JT. Moiré fringes by two spiral gratings and its applications on collimation tests. Chin J Phy 1995;33:439–49.
[20] Yariv A, Yeh P. Optical waves in crystal. Wiley; 1984. p. 84–8.
[21] Chiu MH, Lee JY, Su DC. Complex refractive-index measurement based on Fresnel's equations and uses of heterodyne interferometry. Appl Opt 1999;38:4047–52.